Metal–Organic Frameworks

Time-Resolved In Situ X-ray Diffraction Reveals Metal-Dependent Metal–Organic Framework Formation

Yue Wu, Sebastian Henke, Gregor Kieslich, Inke Schwedler, Miaosen Yang, Duncan A. X. Fraser, and Dermot O'Hare*

Abstract: *Versatility in metal substitution is one of the key aspects of metal-organic framework (MOF) chemistry, allowing properties to be tuned in a rational way. As a result, it important to understand why MOF syntheses involving different metals arrive at or fail to produce the same topological outcome. Frequently, conditions are tuned by trial-and-error to make MOFs with different metal species. We ask: is it possible to adjust synthetic conditions in a systematic way in order to design routes to desired phases? We have used in situ X-ray powder diffraction to study the solvothermal formation of isostructural $M_2(bdc)_2dabco$ (M = Zn, Co, Ni) pillared-paddlewheel MOFs in real time. The metal ion strongly influences both kinetics and intermediates observed, leading in some cases to multiphase reaction profiles of unprecedented complexity. The standard models used for MOF crystallization break down in these cases; we show that a simple kinetic model describes the data and provides important chemical insights on phase selection.*

During the formation of MOFs, the primary chemistry occurs between metal ions and organic ligand functional groups. It is often the case that with a particular ligand system, metals with different chemistries can form isostructural phases. This versatility in metal ion substitution is a key selling point of MOF chemistry, as different metal ions may impart dramatically different functional properties in frameworks of the same topology, while maintaining desirable structural features.[1] It follows that the role of the metal species in framework stability and functionality has been extensively studied.[2] Furthermore, the metal species has a significant effect on a MOF's bulk properties, which then

affects both exploratory research and commercial deployment. For example, certain metal ions such as zinc have a reputation for being more likely to afford large MOF single crystals, making structural analysis much easier; zirconium MOFs on the other hand are notoriously difficult to grow as single crystals.[3]

To date, the most common approach to generating families of MOFs containing different metals is still to start with the conditions used for the parent phase, then tune the conditions through trial and error. A more systematic understanding of the direct influence of different metal ions on MOF crystallization and growth is hence of great importance. A major reason that our understanding of MOF formation lags behind research on their chemical and structural properties, is the technical challenge of interrogating reactions in situ. To date, energy dispersive X-ray diffraction (EDXRD) has been the most commonly used technique[4] but more recently, technological improvements have made angular dispersive XRD (ADXRD) experiments feasible, dramatically increasing the range and resolution of accessible Q-space, as well as increasing time resolution from minutes to seconds.[5–8] Techniques such as SAXS–WAXS (small/wide angle X-ray scattering),[9] XANES (X-ray absorption near-edge spectroscopy),[10] and liquid cell TEM[11] have also been used for in situ MOF studies, but specialized sample environments are required. Herein, we demonstrate the utility of in situ ADXRD in studying laboratory-scale solvothermal reactions (ca. 5–20 mL) with a time resolution of seconds.

An added complication is that the energy landscape of possible MOF phases arising from a reaction mixture is very flat, and hence very dependent on both reaction conditions, and the metal species. In the Al/NH$_2$-bdc system (NH$_2$-bdc = 2-amino-1,4-benzenedicarboxyalte), multiple routes to MIL-53(Al) were observed in situ, including a MOF-235 to MIL-101 different to MIL-53 pathway.[12] The sequential formation of several MOF phases from the same reaction mixture has also been observed in situ for the Fe/bdc[13] (bdc = 1,4-benzenedicarboxylate) and Li/tartrate[5] systems, and ex situ for the V/bdc system.[14]

In order to gain a systematic understanding of the effect of the metal species on MOF growth and phase evolution, we studied the formation of a series of isostructural M_2-(bdc)$_2$dabco (M = Zn, Co, Ni; dabco = diazabicyclo-[2.2.2]octane) pillared-paddlewheel frameworks (PPFs, Figure 1) using time-resolved in situ powder X-ray diffraction (PXRD) at different temperatures.[5,6] The pillared paddlewheel M/bdc/dabco system has been an important platform for MOF research as it provides a simple topology that is very tolerant to metal and ligand substitution.[15–19] The pillared

[*] Dr. Y. Wu, Dr. M. Yang, D. A. X. Fraser, Prof. D. O'Hare
Department of Chemistry, University of Oxford
12 Mansfield Road, Oxford, OX1 3TA (UK)
E-mail: dermot.ohare@chem.ox.ac.uk

Dr. S. Henke, I. Schwedler
Lehrstuhl für Anorganische Chemie II, Ruhr-Universität Bochum
Universitätsstraße 150, 44801 Bochum (Germany)

Dr. G. Kieslich
Department of Materials Science and Metallurgy
University of Cambridge
27 Charles Babbage Road, Cambridge, CB3 0FS (UK)

Dr. M. Yang
Current address:
School of Chemical Engineering, North-east Dianli University
Jilin 132012 (China)

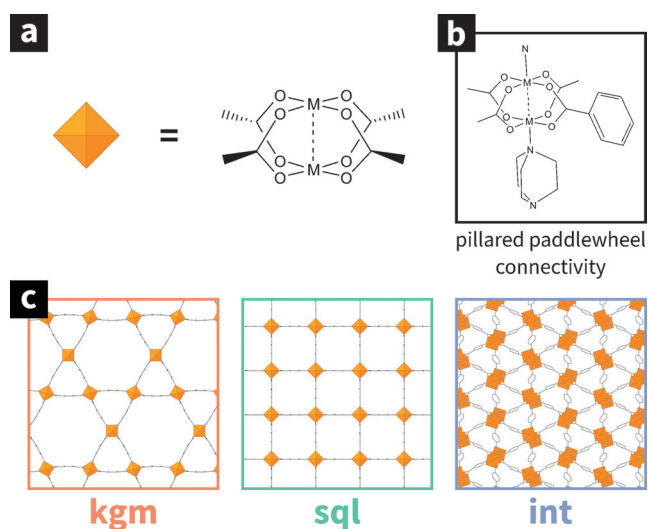Supporting information and the ORCID identification number(s) for the author(s) of this article can be found under http://dx.doi.org/10.1002/anie.201608463.

Figure 1. Schematic representations of a) the $M_2(COO)_4$ paddlewheel motif and b) generalized pillared-paddlewheel framework connectivity. c) Different phases discussed in this paper: the **kgm** and **sql** 2D-layers are based on the binuclear paddlewheel motif pillared in the third dimension, while **int** is based on a trinuclear pinwheel forming a layered 2D-network (**hxl** topology) without 3D connectivity.

Figure 2. Time dependence of the total integrated Bragg scattering and temperature for M/bdc/dabco reactions heated from room temperature with varying metals and set temperatures: a) Co/110°C, b) Co/100°C, c) Zn/120°C, and d) Ni/120°C.

layers most commonly take a square-grid topology (**sql**) but can also exist in a kagome (**kgm**) topology with identical chemical connectivity.[20,21] The layer topology codes **sql** and **kgm** will be used as shorthand for the respective pillared phases. Besides these two paddlewheel (Figure 1 a) based MOF phases, numerous distinct M-bdc[22] and even M-bdc-dabco[23] phases with a trinuclear $M_3(bdc)_6$ "pinwheel" rather than binuclear $M_2(bdc)_4$ paddlewheel motifs exist. We also observe a previously unknown layered intermediate (**int**), which is constructed from sheets of **hxl** connectivity (Figure 1 c).

Using a previously described setup on beamline I12 at the Diamond Light Source (UK),[5,24] we collected in situ PXRD data during the formation of several MOF phases within the M/bdc/dabco system (M = Zn, Co, Ni). In the first experiments, stock solutions of each reagent (M^{2+}, H_2bdc and dabco) were combined stoichiometrically and immediately immersed into a room temperature oil bath with stirring. The oil bath was subsequently heated from room temperature up to 100–120°C (initial heating rate ca. 13°C min^{-1}) while diffraction patterns were recorded with a time resolution of about 1 s. Full details of PXRD data refinement are included in the Supporting Information.

Kondo et al.[20] speculated that in the M/bdc/dabco reaction mixture, triangular oligomers containing three pad-dlewheels in a three-membered ring are kinetically favored over square-shaped oligomers containing four paddlewheels in a four-membered ring, making **kgm** the kinetic PPF product. Our data is consistent with this hypothesis as shown clearly in Figure 2: for all three metal ions, **kgm** is formed first and **sql** crystallizes later whilst **kgm** decays. The contrast between the reaction kinetics of different metals also becomes clear: for reactions containing the more chemically labile Co^{2+} and Zn^{2+} ions,[25] **kgm** is already present at room
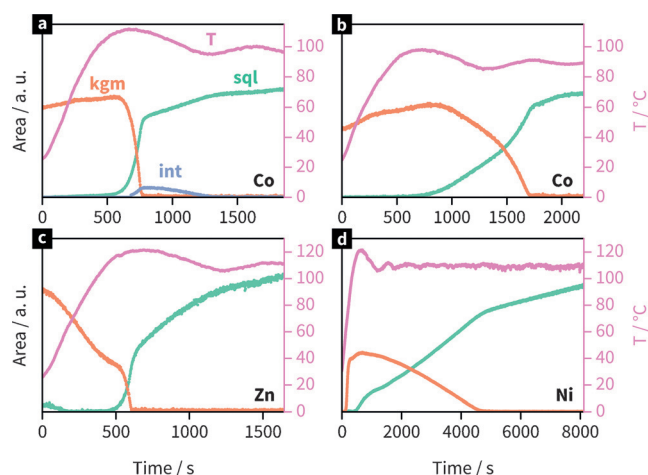
temperature, while Ni-**kgm** is only formed upon heating to ca. 60°C. This is also seen visually—the Co^{2+} and Zn^{2+} reaction mixtures immediately become cloudy after combining the reactants, while the Ni^{2+} reaction mixture remains clear at room temperature. The known higher chemical stability of Ni complexes corresponds to a higher energy barrier to the substitution of existing ligands when in solution.[2] Zn-**kgm** degrades immediately upon heating (Figure 3), which is expected since Zn^{2+} is the most labile of the three metal ions studied here.

In contrast, the Co/bdc/dabco system displays a more complex behavior than its congeners. Co-**kgm** shows growth at lower temperatures prior to its conversion to Co-**sql**. Additionally, a previously unknown Co-**int** phase forms in competition with Co-**sql** in the higher temperature reaction before converting to Co-**sql**. This is discussed further below. Co-**int** can be unambiguously identified as the high-temperature phase of a known layered MOF[22] of composition $Co_3(bdc)_3(DMF)_2(H_2O)_2$ (in situ VT-PXRD of the reversible phase transition of Co-**int** suspended in DMF is shown in the Supporting Information). This phase can be indexed with an orthorhombic unit cell with cell parameters related to the interlayer distance and structural motifs of the reported $Co_3(bdc)_3(DMF)_2(H_2O)_2$ structure, but we were unable to solve the structure. However, this was sufficient to model Co-**int** as a structureless Pawley phase. In our studies, the **int** phase only forms in the Co system. However, the low-temperature phase of Zn-**int** has been previously identified as an impurity in some Zn-**sql** syntheses,[26] showing that the **int** topology is not uniquely formed by Co.

In order to pinpoint the complex phase behavior of these M/bdc/dabco systems, we ran a series of experiments in which the reaction mixtures were made up in the same way but directly immersed into pre-heated oil baths at fixed temperatures. This gave a very stable temperature profile, allowing the observation of reaction kinetics under isothermal conditions (for exact temperature profiles see Figure S2.4). Results from the isothermally heated reactions of the Co/
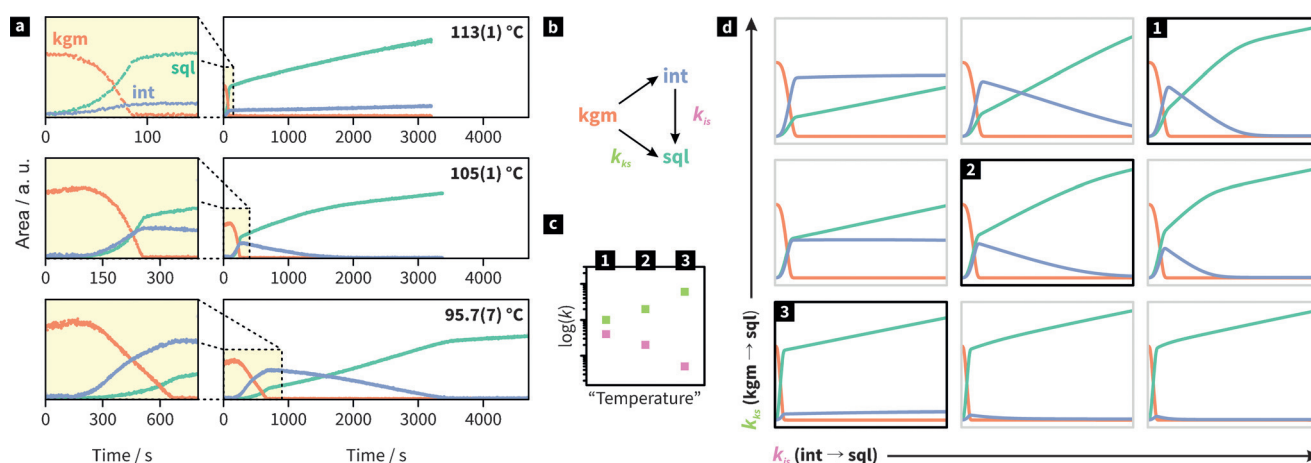
Figure 3. a) Time dependence of total integrated Bragg scattering for the various phases formed in the Co/bdc/dabco system at 95.7(7) °C, 105(1) °C, and 113(1) °C. b) Scheme for the model of the Co/bdc/dabco reaction system used for our kinetic simulations. c) Relative changes in reaction constants and their correspondence to changing reaction temperature. d) Simulated reaction profiles varying two rate constants. (1), (2), and (3) show the corresponding reaction constants in (c) and simulated reaction profiles in (d)—note similarity to the observed profiles in (a).
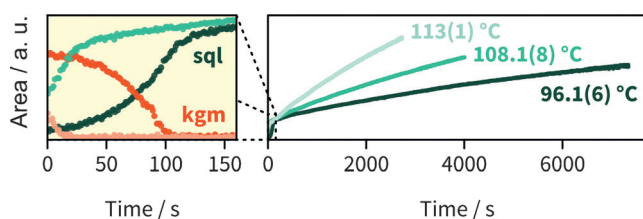

Figure 4. Time dependence of total integrated Bragg scattering for the Zn/bdc/dabco system. Left: Detail of the Zn-**kgm** to Zn-**sql** interconversion at 96.1(6) °C (dark) and 108.1(8) °C (light). Right: Zn-**sql** reaction kinetics at three temperatures; detail is highlighted.

bdc/dabco system are shown in Figure 4a. This system in particular shows a complex reaction profile, with three phases appearing at different times. The reaction profiles for the Co/bdc/dabco system are highly temperature dependent—drastically different behavior is seen in a temperature window of $\Delta T < 20$ °C. We see that as for the from-room-temperature reactions, the **kgm** phase exists at the start of reaction, and has already consumed a large proportion of the reagents. A rapid decay of **kgm** is then accompanied by the growth of **sql** and **int** in competition. Finally, **int** decays with the growth of **sql** (for reactions run at 95.7(7) and 105(1) °C).

The "growth envelope" of the total crystalline content in the reaction appears to increase independently of the phase interconversion processes (see Figure S2.4). This slow growth is particularly clear in the 95.7(7) and 105(1) °C reactions after the **int** phase has fully decayed. It is likely that the slow thermal hydrolysis of DMF gradually occurs and the related increase in pH results in the deprotonation of more H_2bdc over the time of the reaction.[27] It is noteworthy that the complex reaction profile resulting from the multiple phase conversions in the Co/bdc/dabco system cannot be modelled with the Avrami and Gualtieri methods, commonly used to describe crystallization phenomena from solution phase, such as MOF growth.[28] Hence, we developed a minimally parameterized solution kinetic model which captures the key features of the data remarkably well.

Our model based on a total of six equations of two types: 1) The three phase conversion reactions shown in the scheme in Figure 3b, each described by an autocatalytic growth reaction and 2) three simple mass action laws, representing the slow growth of each phase from a large reservoir of reagents in solution (Figure 3b; see Supporting Information for overall details). Essentially, the fundamental features of the phase behavior of the Co/bdc/dabco system can be described by an inverse temperature dependence of the rate constants of conversion for the **int**→**sql** reaction (k_{is}) and the **kgm**→**sql** reaction (k_{ks}) (Figure 3c). The **int** phase gradually converts to **sql** at the two lower reaction temperatures (95.7(7) and 105(1) °C), however, at the highest temperature (113(1) °C) it not only persists but shows positive growth (Figure 4a). This is rationalized in our model where k_{is} (**int**→**sql**) shows negative temperature dependence; coupled with slow growth from solution, this is consistent with the flat/slightly positive profile seen for **int** at 113(1) °C (Figure 3a).

Results from isothermally heated reactions of the Zn/bdc/dabco system are shown in Figure 4. In this system, the **kgm** phase is observed at the two lower temperatures (Figure 4, left) but has a much shorter lifespan than for Co²⁺ (as expected due to the greater lability of Zn²⁺ complexes). At the highest temperature (ca. 113 °C), the **kgm** phase has completely decayed in the time between the start of heating and the start of data collection (ca. 3 min). The subsequent temperature-dependent growth kinetics of Zn-**sql** resemble conventional single-phase MOF growth that has been frequently reported in previous work—higher temperatures result in faster reaction kinetics. Fitting with the Gualtieri model[29] was attempted with the assumption that entire growth profile was single phase, however the data could not be successfully modelled suggesting that, as in the Co/bdc/dabco system, the kinetics are substantially different from those observed for single-phase growth in previous studies.

To conclude: firstly, by using in situ PXRD we are able to rationalize the impact of the metal species on reaction kinetics and intermediate formation in the M_2(bdc)$_2$dabco family of isostructural MOFs. The formation kinetics corre-

spond to the trend in chemical lability of the metal ion used (Zn > Co > Ni). Secondly, we have developed a simple, minimally parametrized method of simulating multiphase MOF growth kinetics. This approach will be of great relevance for the growing area of in situ studies of MOF synthesis. We suggest that further refinement of our model with more data may allow physical meanings to be assigned the model parameters. Unquestionably, understanding of the relationship between metal species, formation kinetics and framework stability is a prerequisite in moving past purely exploratory synthesis to, for example, the targeted synthesis of valuable metastable phases.

[1] T. Grant Glover, G. W. Peterson, B. J. Schindler, D. Britt, O. Yaghi, *Chem. Eng. Sci.* **2011**, *66*, 163–170.
[2] K. Tan, N. Nijem, P. Canepa, Q. Gong, J. Li, T. Thonhauser, Y. J. Chabal, *Chem. Mater.* **2012**, *24*, 3153–3167.
[3] S. Øien, D. Wragg, H. Reinsch, S. Svelle, S. Bordiga, C. Lamberti, K. P. Lillerud, *Cryst. Growth Des.* **2014**, *14*, 5370–5372.
[4] N. Pienack, W. Bensch, *Angew. Chem. Int. Ed.* **2011**, *50*, 2014–2034; *Angew. Chem.* **2011**, *123*, 2062–2083.
[5] H. H.-M. Yeung, S. Wu, S. Henke, A. K. Cheetham, D. O'Hare, R. I. Walton, *Angew. Chem. Int. Ed.* **2016**, *55*, 2012–2016; *Angew. Chem.* **2016**, *128*, 2052–2056.
[6] Y. Wu, M. I. Breeze, G. J. Clarkson, F. Millange, D. O'Hare, R. I. Walton, *Angew. Chem. Int. Ed.* **2016**, *55*, 4992–4996; *Angew. Chem.* **2016**, *128*, 5076–5080.
[7] T. Friščić, I. Halasz, P. J. Beldon, A. M. Belenguer, F. Adams, S. A. J. Kimber, V. Honkimäki, R. E. Dinnebier, *Nat. Chem.* **2013**, *5*, 66–73.
[8] R. I. Walton, F. Millange, *The Chemistry of Metal-Organic Frameworks: Synthesis Characterization, and Applications, Vol. II*, Wiley-VCH, Weinheim, Germany, **2016**.
[9] J. Canivet, A. Fateeva, Y. Guo, B. Coasne, D. Farrusseng, H. Li, M. Eddaoudi, M. O'Keeffe, O. M. Yaghi, S. S. Y. Chui, et al., *Chem. Soc. Rev.* **2014**, *43*, 5594–5617.
[10] M. Goesten, E. Stavitski, E. A. Pidko, C. Gücüyener, B. Boshuizen, S. N. Ehrlich, E. J. M. Hensen, F. Kapteijn, J. Gascon, *Chem. Eur. J.* **2013**, *19*, 7809–7816.
[11] J. P. Patterson, P. Abellan, M. S. Denny, C. Park, N. D. Browning, S. M. Cohen, J. E. Evans, N. C. Gianneschi, *J. Am. Chem. Soc.* **2015**, *137*, 7322–7328.
[12] E. Stavitski, M. Goesten, J. Juan-Alcañiz, A. Martinez-Joaristi, P. Serra-Crespo, A. V. Petukhov, J. Gascon, F. Kapteijn, *Angew. Chem. Int. Ed.* **2011**, *50*, 9624–9628; *Angew. Chem.* **2011**, *123*, 9798–9802.
[13] F. Millange, M. I. Medina, N. Guillou, G. Férey, K. M. Golden, R. I. Walton, *Angew. Chem. Int. Ed.* **2010**, *49*, 763–766; *Angew. Chem.* **2010**, *122*, 775–778.
[14] F. Carson, J. Su, A. E. Platero-Prats, W. Wan, Y. Yun, L. Samain, X. Zou, *Cryst. Growth Des.* **2013**, *13*, 5036–5044.
[15] H. Wang, J. Getzschmann, I. Senkovska, S. Kaskel, *Microporous Mesoporous Mater.* **2008**, *116*, 653–657.
[16] D. N. Dybtsev, H. Chun, K. Kim, *Angew. Chem. Int. Ed.* **2004**, *43*, 5033–5036; *Angew. Chem.* **2004**, *116*, 5143–5146.
[17] P. Maniam, N. Stock, *Inorg. Chem.* **2011**, *50*, 5085–5097.
[18] S. Henke, A. Schneemann, A. Wütscher, R. A. Fischer, *J. Am. Chem. Soc.* **2012**, *134*, 9464–9474.
[19] I. Schwedler, S. Henke, M. T. Wharmby, S. R. Bajpe, A. K. Cheetham, R. A. Fischer, *Dalton Trans.* **2016**, *45*, 4230–4241.
[20] M. Kondo, Y. Takashima, J. Seo, S. Kitagawa, S. Furukawa, *CrystEngComm* **2010**, *12*, 1–11.
[21] H. Chun, J. Moon, *Inorg. Chem.* **2007**, *46*, 4371–4373.
[22] M. Bagherzadeh, F. Ashouri, M. Đaković, *J. Solid State Chem.* **2015**, *223*, 32–37.
[23] H. Chun, H. Jung, G. Koo, H. Jeong, D.-K. Kim, *Inorg. Chem.* **2008**, *47*, 5355–5359.
[24] M. Drakopoulos, T. Connolley, C. Reinhard, R. Atwood, O. Magdysyuk, N. Vo, M. Hart, L. Connor, B. Humphreys, G. Howell, et al., *J. Synchrotron Radiat.* **2015**, *22*, 828–838.
[25] S. Lincoln, *Helv. Chim. Acta* **2005**, *88*, 523–545.
[26] M. Edgar, R. Mitchell, A. M. Slawin, P. Lightfoot, P. A. Wright, *Chem. Eur. J.* **2001**, *7*, 5168–5175.
[27] S. Hausdorf, J. Wagler, R. Mossig, F. Mertens, *J. Phys. Chem. A* **2008**, *112*, 7567–7576.
[28] R. El Osta, M. Feyand, N. Stock, F. Millange, R. I. Walton, *Powder Diffr.* **2013**, *28*, S256–S275.
[29] A. F. Gualtieri, *Phys. Chem. Miner.* **2001**, *28*, 719–728.